Pharm Res (2011) 28:374–385
DOI 10.1007/s11095-010-0282-8

RESEARCH PAPER

The Effect of Crystallizing and Non-crystallizing Cosolutes on Succinate Buffer Crystallization and the Consequent pH Shift in Frozen Solutions

Prakash Sundaramurthi • Raj Suryanarayanan

Received: 23 July 2010 / Accepted: 13 September 2010 / Published online: 7 October 2010

ABSTRACT

Purpose To effectively inhibit succinate buffer crystallization and the consequent pH changes in frozen solutions.

Methods Using differential scanning calorimetry (DSC) and X-ray diffractometry (XRD), the crystallization behavior of succinate buffer in the presence of either (i) a crystallizing (glycine, mannitol, trehalose) or (ii) a non-crystallizing cosolute (sucrose) was evaluated. Aqueous succinate buffer solutions, 50 or 200 mM, at pH values 4.0 or 6.0 were cooled from room temperature to −25°C at 0.5°C/min. The pH of the solution was measured as a function of temperature using a probe designed to function at low temperatures. The final lyophiles prepared from these solutions were characterized using synchrotron radiation.

Results When the succinic acid solution buffered to pH 4.0, in the absence of a cosolute, was cooled, there was a pronounced shift in the freeze-concentrate pH. Glycine and mannitol, which have a tendency to crystallize in frozen solutions, remained amorphous when the initial pH was 6.0. Under this condition, they also inhibited buffer crystallization and prevented pH change. At pH 4.0 (50 mM initial concentration), glycine and mannitol crystallized and did not prevent pH change in frozen solutions. While sucrose, a non-crystallizing cosolute, did not completely prevent buffer crystallization, the extent of crystallization was reduced. Sucrose decomposition, based on XRD peaks attributable to β-D-glucose, was observed in frozen buffer solutions with an initial pH of 4.0. Trehalose completely inhibited crystallization of the buffer components when the initial pH was 6.0 but not at pH 4.0. At the lower pH, the crystallization of both trehalose dihydrate and buffer components was evident.

Conclusion When retained amorphous, sucrose and trehalose effectively inhibited succinate buffer component crystallization and the consequent pH shift. However, when trehalose crystallized or sucrose degraded to yield a crystalline decomposition product, crystallization of buffer was observed. Similarly, glycine and mannitol, two widely used bulking agents, inhibited buffer component crystallization only when retained amorphous. In addition to stabilizing the active pharmaceutical ingredient, lyoprotectants may prevent solution pH shift by inhibiting buffer crystallization.

KEY WORDS buffer crystallization · cosolute · frozen solution · pH shift

P. Sundaramurthi • R. Suryanarayanan (✉)
Department of Pharmaceutics, College of Pharmacy
University of Minnesota
Minneapolis, MN 55455, USA
e-mail: surya001@umn.edu

Present Address:
P. Sundaramurthi
Scientific affairs, Teva Parenteral Medicines Inc.
11 Hughes
Irvine, CA 92618, USA

INTRODUCTION

Freeze-dried formulations are, typically, multi-component systems containing excipients in addition to the active pharmaceutical ingredient (API) (1–4). For example, a freeze-dried protein formulation may contain a buffer, bulking agent, lyoprotectant and surfactant (5). Since a large fraction of APIs are stable only over a narrow pH range, buffering the prelyo solution becomes necessary (6). The selection of a buffer and its concentration are based on desired pH and buffer capacity as well as the possibility of buffer-specific catalysis (7,8). When the prelyo solution is cooled, a potential complication is the pH shift brought about by the selective crystallization of a buffer component.

This has been reported in several buffer systems, though only phosphate buffer systems (sodium and potassium) have been thoroughly investigated.

The pioneering work with phosphate buffer systems was carried out by van den Berg (9,10). The solutions were seeded both with ice and buffer salt to facilitate attainment of equilibrium. The unfrozen liquid was separated from the frozen solid and analyzed. It became evident that as the temperature of the buffer solution was lowered, the disodium phosphate crystallized (9). The pH of the sodium phosphate buffer solution dropped from an initial value of 7.4 at RT to 3.6 at −9.9°C (eutectic temperature). Thus, the selective crystallization of disodium phosphate (basic component) as the dodecahydrate ($Na_2HPO_4 \cdot 12H_2O$) caused a pH change of ~4 units (10).

Such pronounced pH shifts in frozen solutions can be avoided by inhibiting the selective crystallization of a buffer component. We earlier characterized, using synchrotron radiation, the crystallization of sodium phosphate buffer in the presence of glycine (11). When a solution with a 1:3 molar ratio of glycine to sodium phosphate buffer was freeze-dried, buffer component crystallization was completely inhibited in frozen system. On the other hand, at higher molar ratios of glycine to buffer (3:1), there was pronounced glycine crystallization. Pikal-Cleland *et al.* earlier shown that glycine, at low concentrations (≤50 mM), effectively prevents pH change in 10 and 100 mM sodium phosphate buffer (12). However, when the initial glycine concentration was ≥100 mM, buffer salt crystallization was facilitated. While glycine crystallization in frozen buffer solutions was not monitored, they postulated that at lower weight ratios of glycine to buffer, by remaining amorphous, glycine inhibited buffer crystallization. However, at higher weight ratios of glycine to buffer, crystallization of glycine could not be prevented.

In light of the risk of pH shifts in frozen solutions, the use of the phosphate buffer is limited. Since only a small number of buffers are approved for use in parenteral formulations, it is a worthwhile exercise to evaluate the possibility of inhibiting buffer crystallization (5,13). There is obviously a need for other robust buffer systems. In our previous study of succinate buffer, we observed a 'pH swing' in freeze-concentrate due to the sequential crystallization of succinic acid, monosodium succinate, and disodium succinate (14,15). The pH of the solution from the initial value of 4.0 at RT first increased to 8.0 at −25°C and then decreased to 2.5 due to sequential crystallization of buffer components. If a cosolute is retained amorphous, it may inhibit buffer component crystallization and the consequent pH shift. On the other hand, a crystalline cosolute in frozen solutions might facilitate buffer component crystallization. The overall goal of this work is to understand the influence of some commonly used crystallizing and non-crystallizing cosolutes on the crystallization behavior of succinic acid buffer systems in frozen solutions. Our specific objective is to prevent pH shift in frozen solutions through the effective use of cosolutes. While mannitol and glycine were examples of readily crystallizing cosolutes, sucrose and trehalose were the model "non-crystallizing" solutes. We hypothesize that the physical state of the cosolute in frozen solution will influence the crystallization propensity of the buffer components. The solution pH was continuously recorded, both during cooling and annealing. We utilized differential scanning calorimetry (DSC) and X-ray diffractometry (XRD) to monitor crystallization in frozen solutions. In addition, the solutions were freeze-dried, and the lyophiles were characterized using synchrotron radiation.

MATERIALS AND METHODS

Materials

Succinic acid, mannitol, glycine, trehalose dihydrate ($C_{12}H_{22}O_{11} \cdot 2H_2O$), sucrose (all from Sigma) and sodium hydroxide (Mallinckrodt) were purchased with purity >99%. Deionized water was degassed by holding at 70°C for 5 min and membrane filtered (0.45 μm PTFE, Fisher). The degassed water, stored in a closed container at room temperature (RT), was used to prepare buffer solutions. A pH meter (Oakton), calibrated with standard buffer solutions (Oakton standard buffers; pH 2.00, 4.01, 7.00 and 10.00; certified by NIST) was used.

Methods

Preparation of Buffer Solutions

Buffer solutions were prepared by dissolving the appropriate amount of succinic acid and other cosolutes, then adjusting the pH with 2 M NaOH to either 4.0 or 6.0 (± 0.1) at 25°C. The final buffer concentration was either 50 or 200 mM. All the solutions were membrane filtered and stored in tightly closed glass vials at room temperature (RT). Table I lists the buffer solutions investigated in this study.

Lyophilization

Lyophilization was carried out in a bench-top (VirTis® AdVantage™, Gardiner, NY) freeze-dryer. USP Type I borosilicate glass vials (VWR®) with 20 mm neck size and 10 ml fill volume capacity were used. About 5 ml of the buffer solution (initial concentrations 50 and 200 mM; pH values 4.0 and 6.0) either alone or in the presence of

Table I Effect of Cosolutes on Buffer Component Crystallization and Consequent pH Changes after Cooling and Annealing

Initial buffer concentration	Initial pH (pH_{int})	Cosolute (2% *w/v*)	ΔpH^a ($pH_{-25°C} - pH_{int}$)	XRD[b] (frozen solution)	DSC[c] (warming)
200 mM	4.0	none	4.0[d]	SA, NaHSA	Te
		glycine	1.1	β–glycine	No Te
		Mannitol[e]	1.1	amorphous	Te
		sucrose	1.0	β-D-glucose	Te[g]
		trehalose[f]	2.5	amorphous	Te[g]
	6.0	none	−1.7	SA, NaHSA, $Na_2SA{\cdot}6H_2O$	Te
		glycine	0.5	amorphous	No Te
		mannitol	0.3	amorphous	No Te
		sucrose	0.4	amorphous	Tc, Te[g]
		trehalose	0.4	amorphous	Tc, Te[g]
50 mM	4.0	none	0.9	SA, NaHSA	LS
		glycine	0.5	β-glycine	LS
		mannitol	3.7	δ-mannitol	LS
		sucrose	0.1	amorphous	NA
		trehalose	0.0	amorphous	NA
	6.0	none	−1.3	SA, NaHSA, $Na_2SA{\cdot}6H_2O$	LS
		glycine	0.5	β-glycine	LS
		mannitol	0.1	amorphous	NA
		sucrose	−0.1	amorphous	NA
		trehalose	0.1	amorphous	NA

[a] magnitude of pH shift following freezing attributed to selective crystallization of buffer component; [b] crystalline phases identified in the frozen buffer solutions; SA: β–succinic acid; NaHSA: monosodium succinate; $Na_2SA{\cdot}6H_2O$: disodium succinate hexahydrate; [c] the thermal events observed when the frozen solution was heated; Te: eutectic melting; Tc: crystallization; LS: useful information could not be obtained due to low sensitivity; NA: no thermal events of interest were observed; [d] a pH swing was seen (4.0 ➔8.0➔2.2), due to the sequential crystallization of SA, NaHSA and $Na_2SA{\cdot}6H_2O$; [e] while the pH shift indicates crystallization of acidic buffer components (SA, NaHSA), XRD did not reveal this; however eutectic melting was observed in DSC; [f] Crystallization of trehalose (as trehalose dihydrate) and SA was observed on prolonged annealing; these results were presented in an earlier publication (26); [g] explained in the text

cosolute was filled in glass vials and then loaded into the freeze-dryer. The shelf was cooled to −50°C at 0.5°C/min, held for 1.5 h, heated to −25°C and held for 4 h. Following this annealing step, primary drying (at 60 mTorr) was carried out at a shelf temperature of −30°C for 30 h. Secondary drying was conducted, first at −10°C for 3 h and then at 10°C for 5 h. At the end of the cycle, the vials were capped with rubber stoppers (two-leg gray butyl, Fisher Scientific) under dry nitrogen purge and stored at RT.

Temperature and pH Measurements During Cooling

About 25 ml of solution was placed in a jacketed beaker (100 ml) connected to a water bath with an external controller unit (Neslab RTE 740, Thermo electron, NH). A low temperature pH electrode (Inlab®cool, Mettler Toledo, Switzerland) was placed in the center of the sample and connected to a pH meter (pH 500 series, Oakton, Singapore) to monitor the electromotive force (EMF), from which the pH of the solution was calculated. Initially, the solutions were allowed to equilibrate at 0°C, and then cooled to −25°C at 0.5°C/min. The full experimental details were provided in our earlier publication, and the relevant specific details are given in the figure legends (14,16).

X-Ray Diffractometry (XRD)

A powder X-ray diffractometer (Model XDS 2000, Scintag; Bragg-Brentano focusing geometry) with a variable temperature stage (High-Tran Cooling System, Micristar, Model 828D, R.G. Hansen & Associates; working temperature range: −190 to 300°C) and a solid-state detector was utilized for low temperature XRD studies. The samples were exposed to Cu Kα radiation (45 kV×40 mA), and the XRD patterns were obtained by scanning over an angular range of 5 to 35° 2θ with a step size of 0.05° and a dwell time of 1 s.

About 1 ml of prelyo solution was placed in an aluminum sample holder and covered with a stainless steel dome with a beryllium window. The sample holder was then cooled at 1°C/min, from RT to −10°C, where the first XRD pattern was collected. The sample temperature was decreased to −24°C at a step size of 2°C, and at every step an isothermal XRD pattern was collected. Finally, the frozen solution was annealed at −25 C for 1 h.

Analysis of the final lyophilies was performed at the synchrotron beam line 6-ID-B of the Midwest Universities Collaborative Team's Sector 6 at the Advanced Photon Source, Argonne National Laboratory (Lemont, IL, USA). More details of the instrumental setup, experimental conditions and data analysis are provided in our earlier publications (11,15,17).

Differential Scanning Calorimetry (DSC)

A differential scanning calorimeter (MDSC, Model 2920, TA instruments, New Castle, DE) equipped with a refrigerated cooling accessory was used. About 10 mg of sample was weighed in an aluminum pan and hermetically sealed. The solutions were cooled from RT to −50°C, held for 15 min, and warmed to RT. The heating and cooling rates were 1°C/min. Dry nitrogen gas was purged at 50 ml/min. Data were analyzed using software provided with the instrument (Universal Analysis® 2000).

RESULTS AND DISCUSSION

The 'as-received' materials were characterized by XRD and DSC. The succinic acid, glycine, and mannitol were identified, respectively, as the β-, α- and δ-polymorphic forms (all anhydrous). Succinic acid is a dicarboxylic acid with pKa values of 4.21 and 5.64 at RT, and it is typically used to buffer solutions in the pH range of 3.2 to 6.5. We prepared the succinic acid solutions and buffered to pH values 4.0 and 6.0 using NaOH solution.

The crystalline buffer components—succinic acid, monosodium and disodium succinate—were identified based on their characteristic XRD peaks. The anhydrous β-succinic acid was characterized by peaks (Cu Kα radiation; λ =1.5407Å) at 20.1° (4.41Å) and 26.0° 2θ (3.42Å). Monosodium succinate exhibited unique peaks at 14.0° (6.32Å) and 17.8° 2θ (4.98Å), while the characteristic peak of disodium succinate was observed at 11.9° 2θ (7.43 Å).

Succinate Buffer Crystallization and Consequent "pH Swing"

Previous studies, as discussed earlier, demonstrated the sequential crystallization of buffer components and the consequent "pH swing" when an aqueous succinate buffer solution (200 mM; RT) was cooled to −25°C (14,15). However, the addition of cosolutes can influence the crystallization behavior and the consequent pH shifts in frozen buffer solutions (18). We therefore investigated the crystallization propensity of succinate buffer components in the presence of each of the following: glycine, mannitol, sucrose and trehalose—the four commonly used cosolutes in lyophilized formulations.

Table I lists the magnitude of pH change upon cooling succinate buffer solutions of different initial concentrations and pH values. When a 200 mM succinate, buffered to pH 4.0 was cooled from RT to −25°C, due to the sequential crystallization of buffer components, the pH initially increased (4.0 to 8.0) and then decreased (8.0 to 2.5). A similar 'pH swing' (6.0 to 4.3 to 5.6), but in the opposite direction, was observed when the succinate buffer with an initial pH value of 6.0 was cooled. The magnitude and direction of pH shift were dependent on the initial buffer concentration and pH.

Effect of Glycine

Figure 1 provides the pH of the succinate buffer solution (containing glycine) as a function of temperature, as the solution was cooled and held at −25°C. Solutions with initial concentrations of 50 and 200 mM were buffered to pH values 4.0 (panel a) and 6.0 (panel b). The pH change during cooling was negligible until ice crystallized at ~ −8.0°C. The release of the latent heat of crystallization resulted in a sudden increase in sample temperature to ~ 0°C.

When the solution containing succinate buffer (200 mM; pH 4.0) and glycine (2% *w/v*) was cooled to −25°C, and held for 60 min, the increase in freeze-concentrate pH was much less (1.1 units) than that in the absence of glycine (4.0 units) (Fig. 1, panel 1; Table I). The effect of glycine persisted when the buffer concentration decreased to 50 mM (Table I). Glycine, by inhibiting buffer component crystallization, attenuated the pH changes in the freeze-concentrate. However, when the glycine concentration was increased (4% *w/v*), there were an initial sharp increase in the pH to ~ 7.4, followed by a rapid decrease to ~ 2.6, and finally an increase to 8.4 (data not shown). We speculate sequential crystallization of succinic acid, monosodium succinate, disodium succinate and glycine. The solubility values of succinic acid and glycine are known over the temperature range of 60 to 0°C, and we linearly extrapolated these to −25°C. Our speculation is based on the estimated solubility at this temperature (19).

Similar experiments were also performed with solutions buffered to pH 6.0 (Fig. 1; panel 2). Irrespective of the initial buffer concentration (50 and 200 mM), in the presence of glycine (2% *w/v*), only a small pH increase (~ 0.5 units) was observed. At pH 6.0, disodium succinate is the predominant species and its crystallization would cause the pH to decrease as was observed in the absence of glycine (Table I). However, we observed only a small increase in the freeze-concentrate pH (~ 0.5 units) and no evidence of solute crystallization. A similar effect was

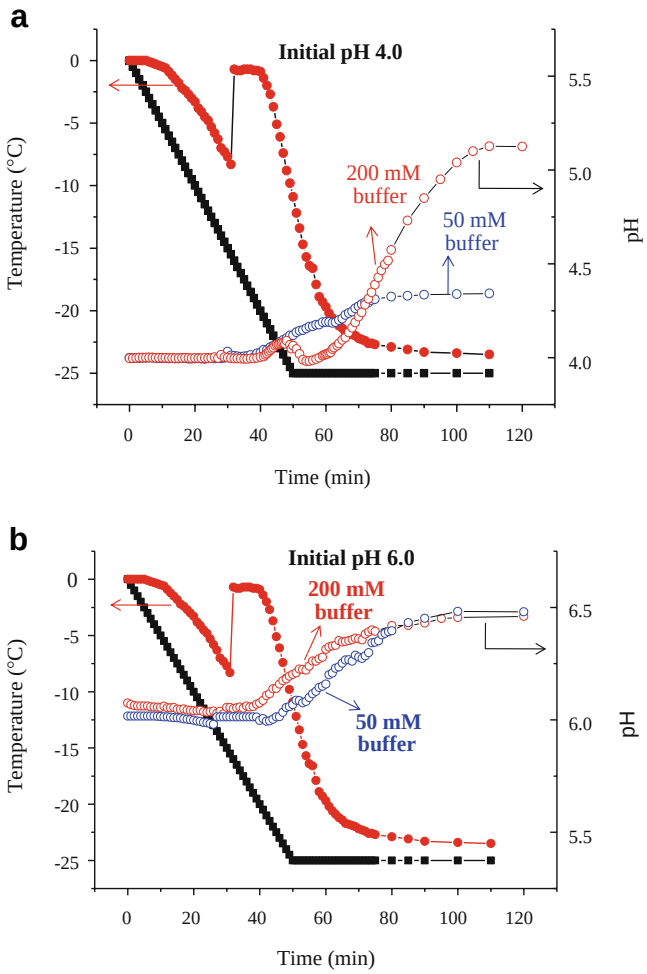

Fig. 1 Low temperature pH measurement of aqueous succinate buffer (50 or 200 mM) solution containing glycine (2% *w/v*) during cooling, followed by isothermal hold at −25°C. Representative bath (−■−) and sample (−●−) temperatures are also given. The solutions had been buffered to pH values of 4.0 (panel a), and 6.0 (panel b) at RT.

observed even when the glycine concentration was increased to 4% *w/v*. This indicated that glycine (≤ 4% *w/v*) inhibited the buffer component crystallization in frozen succinate with an initial pH of 6.0.

The effectiveness of glycine at low concentration (≤ 2% *w/v*) was more pronounced when the buffer concentration was high (200 mM). At low buffer concentration (50 mM), glycine prevented the pH change only in solutions buffered to pH 6.0, but not to pH 4.0. The pH shift in frozen succinate buffer (50 mM; pH 4.0) solution was 0.9 units (Table I), as compared to 0.5 units in the presence of glycine (Fig. 1 panel 1). We attribute this effect to the mutual inhibition of both glycine and buffer components' crystallization in frozen solutions. In other words, buffer salts inhibited the crystallization of glycine, which in turn retarded the buffer crystallization. This was investigated further using XRD. There was no evidence of buffer crystallization in the annealed frozen solution (Fig. 2). However, the characteristic peaks of β-glycine were observed even when the glycine concentration was only 2%, as long as the buffer concentration was low (50 mM). At a higher buffer concentration (200 mM), glycine crystallization was evident only when the glycine concentration was at least 4% and only in solutions buffered to pH 4.0.

Figure 3 shows the DSC heating curves of frozen buffer (200 mM) solution with an initial pH value of 4.0 (panel a) or 6.0 (panel b). The solution buffered to pH 4.0 (in the absence of glycine) revealed two endotherms at −8.9 and −4.1°C before ice melting at −2.2°C (panel a). When the initial pH was 6.0, multiple endotherms were observed in the temperature range of −13.0 to −9.0°C (panel b). The assignments of these peaks were discussed in our earlier publication (15). When solutions containing glycine alone were cooled from RT to −50°C, ice crystallized at −13.3°C, followed by solute crystallization at −22.1°C (data not shown). During warming, there was eutectic melting at −3.6°C and ice melting at −1.2°C. This is in excellent agreement with the reported eutectic temperature of −3.5°C (20–24).

When the frozen buffer solutions (pH 4.0 or 6.0) containing glycine (2% *w/v*) were warmed, no eutectic melting was observed. However, when the glycine concentration was increased to 4%, endotherms attributable to melting were observed at −7.6°C (initial pH 4.0) and at −13.2 and −8.1°C (initial pH 6.0). This is likely to be the eutectic melting of buffer components (20–24). In these samples, as the ice started to melt at ~−3.8°C, eutectic melting of glycine-ice was not discernable.

Effect of Mannitol

The eutectic temperature of mannitol-ice binary system is reported to be −1.5°C (25,26). In this study, when the frozen aqueous mannitol solution (2% *w/v*) was warmed in the DSC pan, a peak attributable to the eutectic melting was observed at ~−1.3°C. This occurred as a shoulder with the ice melting peak. XRD of the annealed frozen solution at −25°C revealed the characteristic peaks of ice and δ-mannitol (data not shown).

When a 200 mM buffer solution containing mannitol (2% *w/v*) with an initial pH value of 4.0 was cooled, there was a gradual increase in pH to 5.1 (Fig. 4 panel a). In contrast, a pronounced increase (3.7 units) in freeze-concentrate pH was observed upon cooling a 50 mM buffer (pH 4.0) solution containing mannitol (2% *w/v*) to −25°C. In the absence of any cosolute, the magnitude of pH change (50 mM, pH 4.0) was only 0.9 units. When the buffer concentration was low (50 mM), the magnitude of pH shift in presence of mannitol (3.7 units) was comparable with the pH shift observed in solution of high buffer concentration without a cosolute. This effect was attributed to crystallization of mannitol enhancing the buffer crystal-

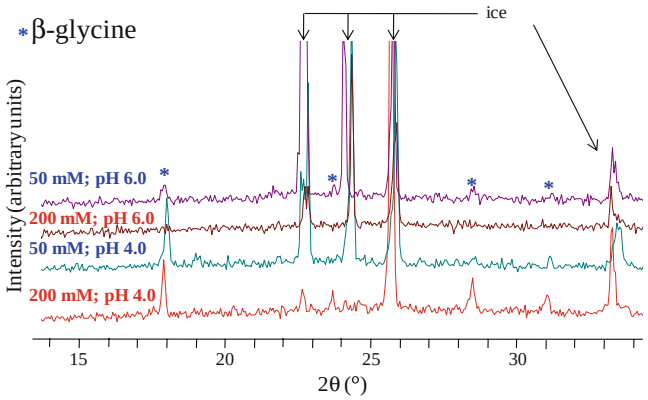

Fig. 2 XRD patterns of frozen aqueous solutions containing glycine (2% *w/v*) and succinate buffer with different initial pH values (4.0 and 6.0). The samples were initially cooled from RT to −10°C, held for 10 min, and then cooled to −24°C while collecting XRD pattern (isothermal hold for 10 min) at each 2°C interval. Finally, the sample was annealed at −25°C for 70 min. Only the XRD pattern collected at the end is provided. The characteristic peaks of β–glycine and hexagonal ice are indicated (33).

lization. XRD (Fig. 5) revealed δ–mannitol crystallization only in 50 mM solutions (pH 4.0). However, there was no evidence of buffer component crystallization. Even if there is crystallization from this buffer solution, it could be below the detection limit of XRD. The frozen buffer solutions (with mannitol) of all other concentrations and pH values, except 50 mM and pH 4.0, showed no solute crystallization. The DSC heating curve of the frozen buffer solution (200 mM and pH 4.0) consisted of an endotherm at ~−10°C. At this low temperature, it is likely to be the eutectic melting of a buffer component (Fig. 6).

On the other hand, in solutions (both 50 and 200 mM) buffered to pH 6.0, there was only a small change in the pH upon cooling to −25°C. In comparison with the buffer solutions without mannitol (Table 1), the magnitude of pH change observed in the presence of mannitol was much less. Both XRD and DSC did not reveal solute crystallization. Mannitol appeared to be effective in inhibiting buffer crystallization when the initial pH value was 6.0. Thus, pH measurement appeared to be a sensitive indicator of buffer crystallization, while DSC and XRD were excellent complementary techniques.

Effect of Trehalose and Sucrose

In the previous section, we observed that there was a mutual crystallization inhibition of both buffer components and cosolute (mannitol and glycine). The influence of non-crystallizing cosolutes on the buffer component crystallization was evaluated using trehalose and sucrose.

When a buffer solution (200 mM, pH 4) containing trehalose (2% *w/v*) was cooled to −25 C, there was a gradual increase in freeze-concentrate pH to 6.5 (Fig. 7). A similar but less pronounced pH shift was seen in the presence of sucrose (4.0 to 5.0). However, at low initial buffer concentration (50 mM), there was no significant change from the initial pH value of 4.0 (Table I).

In light of their ability to remain amorphous in frozen solutions, non-crystallizing solutes are known to inhibit buffer crystallization (12,27). However, the increase in the freeze-concentrate pH in the presence of sucrose and trehalose was counter-intuitive. In an effort to explore this further, these frozen solutions were investigated using DSC (Fig. 8) and XRD (Fig. 9).

The DSC heating curve of frozen aqueous buffer solutions (200 mM, pH 4.0) containing either sucrose (−13.6 and −4.3°C) or trehalose (−11.0 and −4.1°C) showed two weak endotherms, indicating solute crystallization (Fig. 8 panel 1). Based on the thermal behavior of frozen succinate buffer solution, the first endotherm (−13.6 and −11.0°C) was attributed to the melting of (monosodium succinate+ice) eutectic, while the second endotherm

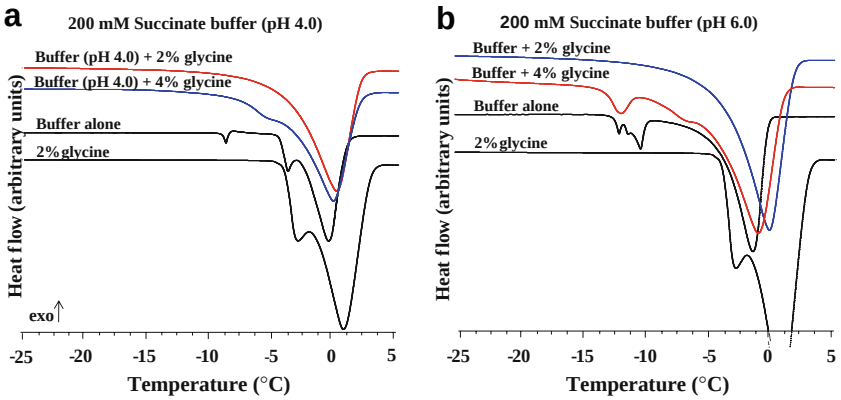

Fig. 3 DSC heating curves of frozen aqueous solutions containing glycine (2% or 4% *w/v*) and succinic acid buffer (200 mM). The solutions had been buffered to pH values of 4.0 (panel a) and 6.0 (panel b) at RT. As a control, DSC heating curves of frozen aqueous buffers solution (200 mM) and glycine (2% *w/v*) solution alone are also given. The solutions were initially cooled from RT to −50°C, held for 15 min, and warmed back to RT. Both the heating and cooling rates were 1°C/min. Only a portion of the final heating curve is provided.

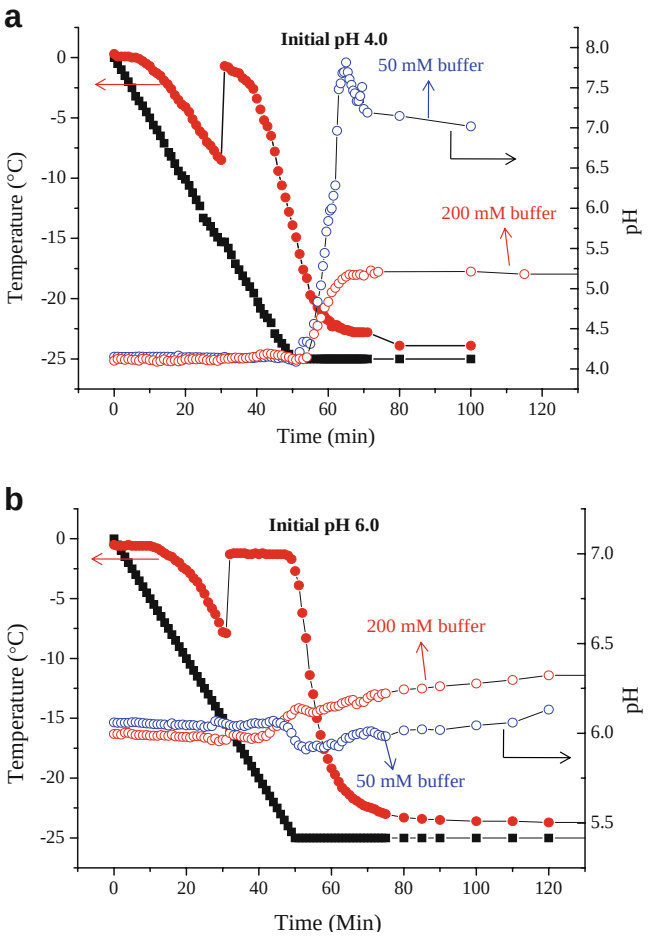

Fig. 4 Low temperature pH measurement of aqueous succinate buffer (50 or 200 mM) solution containing mannitol (2% *w/v*) during cooling followed by isothermal hold at −25°C. Representative bath (−■−) and sample (−●−) temperatures are also given. The solutions had been buffered to pH values of 4.0 (panel a), and 6.0 (panel b) at RT.

(−4.3 and −4.1°C) to that of (succinic acid+ice) eutectics (15). The crystallization of these acidic buffer components explains the increase in the freeze-concentrate pH. The barely discernible endotherms reflect the pronounced inhibition of crystallization brought about by the non-crystallizing cosolutes. In an effort to directly detect solute crystallization, XRD patterns of frozen and annealed buffer solutions were obtained (Fig. 9). In the presence of sucrose or trehalose, there was no evidence of solute crystallization. Thus, in this case, DSC appeared to be a more sensitive indicator of buffer crystallization than XRD.

Similar experiments were also performed with solutions buffered to pH 6.0 (Fig. 8 panel 2). In the frozen buffer solution without a cosolute, sequential crystallization of the basic and acidic buffer components resulted in a pH swing (14,18). In contrast, in the presence of either sucrose or trehalose, there was no pH shift (Table I). However, the DSC heating curve of the frozen buffer solution containing sucrose showed a broad exotherm (between −24.2 and −17.2°C) and

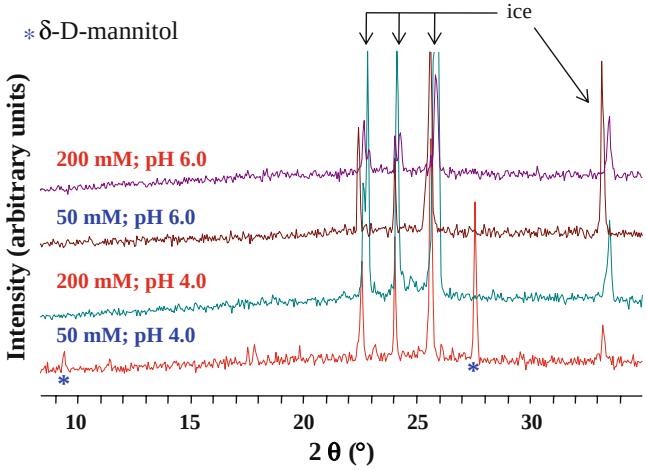

Fig. 5 XRD patterns of frozen aqueous solutions containing mannitol (2% *w/v*) and succinate buffer with different initial pH values (4.0 and 6.0). The samples were initially cooled from RT to −10°C, held for 10 min, and then cooled to −24°C while collecting XRD pattern (isothermal hold for 10 min) at each 2°C interval. Finally, the sample was annealed at −25°C for 70 min. Only the XRD pattern collected at the end is provided. The characteristic peaks of β–D-mannitol and hexagonal ice are indicated (33).

an endotherm (−11.0°C). Similarly, trehalose containing frozen buffer solution also showed a broad exotherm (between −28.3 and −14.4°C) and an endotherm (−11.3°C). While the exotherm is attributed to solute crystallization, the endotherm is due to melting of disodium succinate-ice eutectic. The buffer components were retained amorphous in the freeze-concentrate during cooling, but upon warming disodium succinate crystallized and melted as a eutectic with ice. This indicated that in the presence of non-crystallizing cosolutes, there was an increased resistance to buffer crystallization. As discussed earlier, XRD of solution cooled to −25°C revealed no solute crystallization (Fig. 9 panel a). However, synchrotron XRD revealed the crystallization of acidic buffer components and trehalose dihydrate (18,26). As expected, DSC heating curves of frozen aqueous trehalose and sucrose solutions revealed only glass transition events in the range of −33 to −31°C (data not shown).

If there is a decrease in pH brought about by buffer crystallization, the highly acidic environment could trigger sucrose hydrolysis. In light of the low temperature and the short experimental timescales, the product (glucose and fructose) concentration is expected to be low. Indeed, several weak peaks attributable to β–D-glucose were observed (Fig. 9).

Effect of Cosolutes on pH Change in Frozen Buffer Solutions

High Buffer Concentration (200 mM)

The ability of cosolutes to inhibit succinate buffer components' crystallization in frozen solution can be rank-ordered based on the attenuation in pH shift.

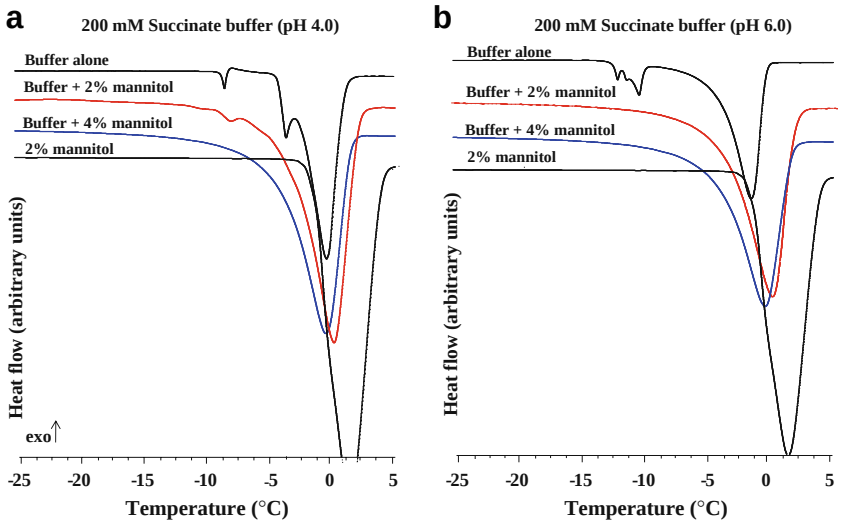

Fig. 6 DSC heating curves of frozen aqueous solutions containing mannitol (2% or 4% *w/v*) and succinic acid buffer (200 mM). The solutions had been buffered to pH values of 4.0 (panel a) and 6.0 (panel b) at RT. As a control, DSC heating curves of frozen aqueous buffers solution (200 mM) and mannitol (2% *w/v*) solution alone are also given. The solutions were initially cooled from RT to −50°C, held for 15 min, and warmed back to RT. Both the heating and cooling rates were 1°C/min. Only a portion of the final heating curve is provided.

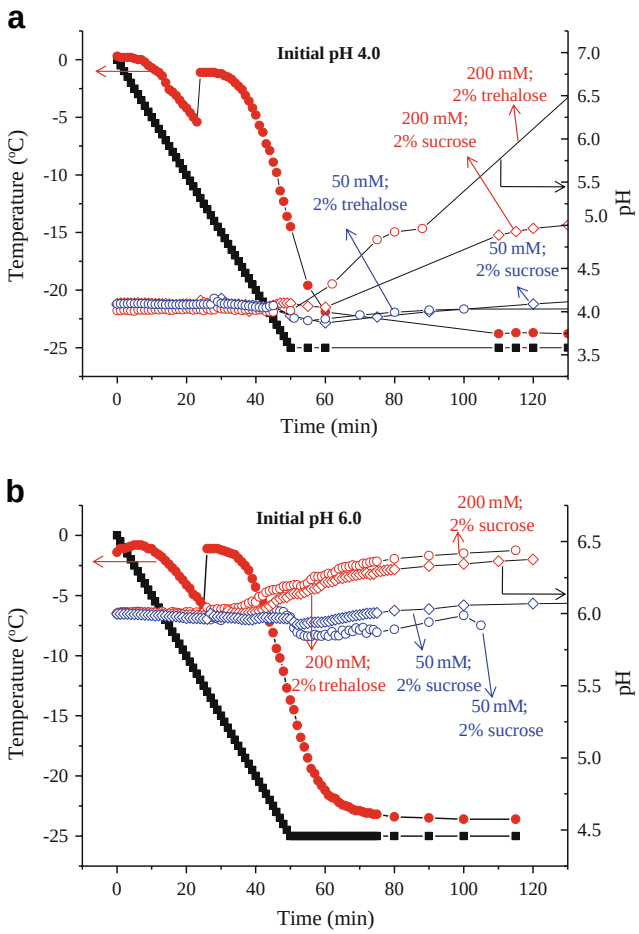

Fig. 7 Low temperature pH measurement of aqueous solution containing sucrose or trehalose (2% *w/v*) and succinate buffer during cooling, followed by isothermal hold at −25°C. Representative bath (−■−) and sample (−●−) temperatures are also given. The solutions had been buffered to pH values of 4.0 (panel a), and 6.0 (panel b) at RT.

Initial pH 4.0

Irrespective of the cosolute, when the initial buffer concentration was high, significant pH shift was observed. However, when compared to the buffer system without a cosolute, the pH shift in frozen solution was effectively attenuated by glycine, mannitol and sucrose, but not trehalose (Figs. 1, 4, and 7, Table I). The pH shift in the presence of crystallizing cosolutes (glycine and mannitol) was ~1.2 units. It is interesting to note that the corresponding XRD showed the crystallization of only glycine, but not mannitol. Crystallization of glycine has been reported to be dependent on the pH of the solutions (11,17). The increase in pH due to buffer component crystallization, by altering the speciation of glycine, prevented further crystallization of glycine. The remaining uncrystallized fraction of glycine in turn inhibited further crystallization of buffer components.

While the pH shift in the presence of crystallizing cosolutes is not surprising, the behavior in presence of non-crystallizing cosolutes warrants further investigation. At pH 4.0, succinic acid, the least soluble buffer species, is predominantly unionized. This is likely to result in a higher degree of supersaturation in frozen solutions and hence greater propensity for crystallization (28). Thus, readily crystallized succinic acid induced the crystallization of trehalose dihydrate, which in turn facilitated further crystallization of buffer component. Similarly, *in situ* seeding-induced crystallization of trehalose dihydrate was reported in trehalose-mannitol frozen aqueous solutions (26). Chemical degradation of sucrose, followed by the crystallization of glucose (one of the degraded products) from acidic (pH 4.0) buffer solutions explains the inability of sucrose to inhibit buffer crystallization.

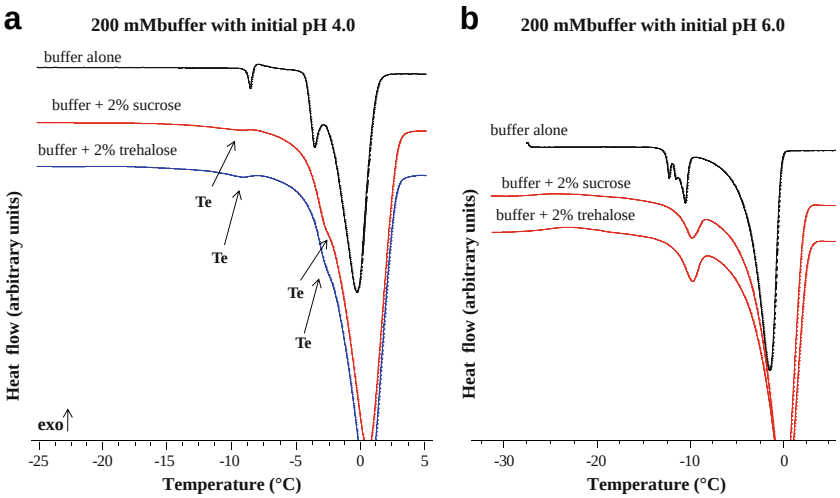

Fig. 8 DSC heating curves of frozen aqueous solutions containing sucrose or trehalose (2%) and succinic acid buffer (200 mM). The solutions had been buffered to pH values of 4.0 (panel a) and 6.0 (panel b) at RT. The solutions were initially cooled from RT to −50°C, held for 15 min, and warmed back to RT. Both the heating and cooling rates were 1°C/min. Only a portion of the final heating curve is provided.

Initial pH 6.0

On the other hand, upon cooling the solutions buffered to pH 6.0, irrespective of the solute (crystallizing or non-crystallizing), only a very small pH shift was observed. This is not likely to be due to selective crystallization of a buffer component. At pH>pKa_2, the buffer would exist predominantly as the completely deprotonated succinate ion (A^{2-}). The crystallization of disodium succinate will cause the freeze-concentrate pH to decrease. Since such a decrease was not observed, the cosolutes effectively inhibited buffer component crystallization and prevented subsequent pH

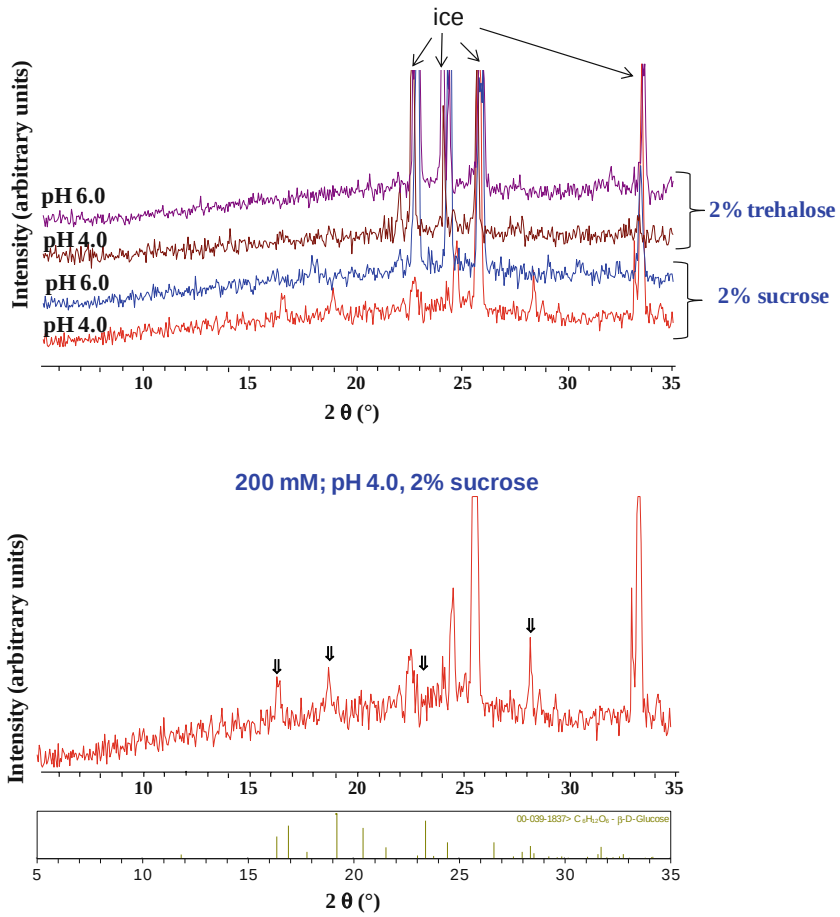

Fig. 9 Overlaid XRD patterns of solutions containing succinate buffer (200 mM) and either sucrose or trehalose (2%) upon freezing to −25°C. The solutions were initially cooled from RT to −10°C at 1°C/min. The first XRD pattern was collected at −10°C, and subsequently the patterns were collected at every 2°C increment. The bottom XRD pattern from the upper panel is shown separately in the lower panel. For comparison purposes, the stick pattern of β-D-glucose obtained from the Powder Diffraction Files of the International Centre for Diffraction Data are provided (33).

shift. Such a mutual inhibition of crystallization was also reported in mannitol–NaCl and glycine–sodium phosphate buffer systems (11,29).

Low Buffer Concentration (50 mM)

Upon freezing the solution (50 mM) buffered at pH 4.0, in the absence of cosolutes, the pH shift was only 0.9 units (Table I). In the presence of cosolutes, except mannitol, there was an appreciable attenuation in the freeze-concentrate pH shift. In the presence of mannitol, there was a pronounced increase in freeze-concentrate pH (~3.7 units). Such a pronounced increase (~4.0 units) was observed only when the buffer solution with a high initial concentration (200 mM) without cosolutes was cooled. At the higher pH value (6.0), irrespective of the cosolute, the observed pH shift was small (≤ 0.5 units). However, this was not the case when the initial solution pH was 4.0 (both high and low buffer concentrations). Hence, our discussion will now be restricted to solutions buffered to pH 4.0.

In the presence of mannitol, the pH shift upon cooling the 200 mM solution buffered to pH 4.0 was much less than that of the 50 mM solution. Based on XRD, crystallization of δ-mannitol was evident only when the buffer concentration was low (50 mM). Obviously, mannitol crystallization enhanced buffer crystallization and caused a pronounced pH shift. The crystallization of mannitol only in the solution with low buffer concentration is intriguing. This could be attributed to the difference in the molar ratio of Na^+ to mannitol. At the higher buffer concentration (200 mM), the molar ratio of Na^+ to mannitol was 0.7, while it was 0.2 at the lower (50 mM) buffer concentration. Crystallization of mannitol in frozen solution was reported to be effectively inhibited by sodium chloride (29,30). When compared with a series of additives including PVP and alditols, NaCl was the most effective crystallization inhibitor. Izutsu *et al.* observed an increase in intermolecular hydrogen bonding and a decrease in intramolecular hydrogen bonding following addition of Na^+ to sorbitol, an isomer of mannitol (31,32).

A similar mechanism may be operative in effectively inhibiting mannitol crystallization. Obviously this effect is expected to be more pronounced at higher molar ratios of Na^+ to mannitol (200 mM; pH 4.0). While crystallization of mannitol was observed only in the 50 mM (pH 4.0) solution, the pronounced increase in pH shift indicates buffer crystallization as well. Thus, at the lower ratio of Na^+ to mannitol, crystallization of both buffer and cosolute occurred.

The effect of glycine in the solution buffered to pH 4.0 was difficult to explain, since β-glycine crystallized at both buffer concentrations. At the higher concentration (200 mM), the observed pH shift (1.1 units) was much higher than that (0.5 units) at lower buffer concentration. Earlier, using synchrotron radiation, we investigated the crystallization of both glycine and sodium phosphate buffer components in frozen solutions. At a glycine-to-sodium phosphate ratio of 50:17 (mM), buffer crystallization was completely inhibited. However, when the buffer concentration was increased to 50 mM, without altering glycine concentration (50 mM), the buffer crystallization was observed (11).

In summary, whenever the cosolute remained amorphous, buffer crystallization was inhibited. In other words, the cosolute, by remaining amorphous, inhibited buffer component crystallization. When trehalose crystallized (pH 4.0, 200 mM), there was a pronounced pH shift reflecting buffer salt crystallization. While sucrose did not crystallize, it degraded, and one of the degraded products (glucose) crystallized. This was also accompanied by a pH shift.

We set out to determine the effect of cosolutes on buffer component crystallization. Our results indicate that while each cosolute influenced buffer component crystallization, the buffer components, in turn, influenced the crystallization behavior of the cosolute.

Characterization of the Final Lyophile

Though there was a pronounced pH change upon cooling the buffer solutions containing a cosolute, direct evidence of buffer component crystallization was not evident in XRD (laboratory source). In an effort to enhance sensitivity, selected experiments were performed using a synchrotron radiation. This also enabled us to link the pH changes observed in frozen solutions to crystalline buffer components in the final lyophiles (Figs. 10 and 11).

All the lyophiles were crystalline, except when the buffer solution (pH 6.0) was freeze-dried in the presence of trehalose. When the initial pH was 4.0, irrespective of the cosolute, the lyophiles contained both succinic acid and monosodium succinate. The lyophile prepared from solution buffered to pH 6.0 contained disodium succinate and traces of succinic acid. Glycine and mannitol had readily crystallized in the final lyophile as their respective β- and δ-anhydrous forms. When the initial pH was 4.0, the lyophile prepared with trehalose contained D-trehalose dihydrate. At both pH values, the lyophiles in the presence of sucrose composed of β-D-glucose. The acidic pH shift due to buffer component crystallization resulted in the decomposition of sucrose and formation of glucose.

Significance and Practical Implications

Selective crystallization of a buffer component, by causing a pronounced shift in the freeze-concentrate pH can

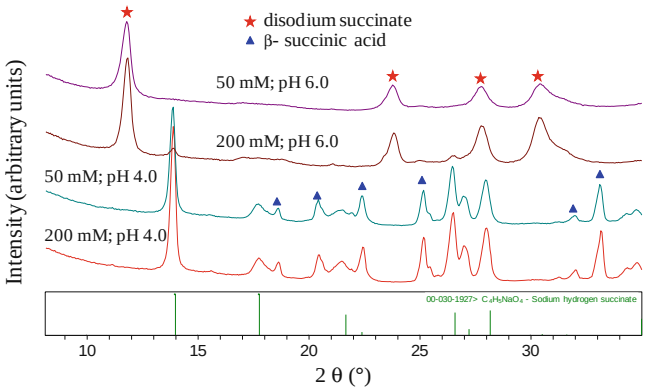

Fig. 10 XRD patterns of final lyophiles prepared using succinate buffer (50 or 200 mM) solution with initial pH values of 4.0 and 6.0. The characteristic peaks of disodium succinate and β-glycine are pointed out. For comparison purposes, the stick pattern of monosodium succinate obtained from the Powder Diffraction Files of the International Centre for Diffraction Data is provided (33).

adversely affect the chemical stability of the API. The magnitude and direction of pH change brought about by buffer component crystallization became evident from low temperature pH measurement. DSC and XRD not only aided us in understanding the phase behavior of the systems, but also enabled the identification of the crystallizing species. This underscores the importance of utilizing complementary techniques to characterize the complex multi-component systems of pharmaceutical interest.

The crystallization behavior of the buffer component could be modulated through cosolutes. When mannitol crystallized readily, a pronounced pH shift was observed, reflecting pronounced buffer component crystallization. Interestingly, when the initial buffer concentration was high (200 mM), crystallization of buffer component induced trehalose crystallization, known to be a non-crystallizing solute. Thus, the cosolute influenced the crystallization of buffer component and *vice versa*.

We did not evaluate the effect of active pharmaceutical ingredients on the crystallization behavior of the buffer components. However, from our results, it is obvious that much like the cosolute, the physical form of the API in the frozen system can influence the phase behavior of the excipients and *vice versa*.

CONCLUSIONS

The effect of crystallizing and non-crystallizing cosolutes on the phase behavior of succinate buffer in frozen and freeze-dried systems was investigated. In solutions buffered to pH 6.0, crystallization of bulking agents such as glycine and mannitol was inhibited in frozen systems. These amorphous cosolutes, in turn, inhibited buffer component crystallization and the consequent pH shift. As expected, trehalose and sucrose by remaining amorphous, also effectively inhibited buffer crystallization. At a lower pH value of 4.0, crystallization of both trehalose dihydrate and buffer components (succinic acid and monosodium succinate) occurred with an attendant pH shift. Degradation of sucrose in frozen buffer solution was evident from the appearance of peaks attributable to crystalline β-D-glucose.

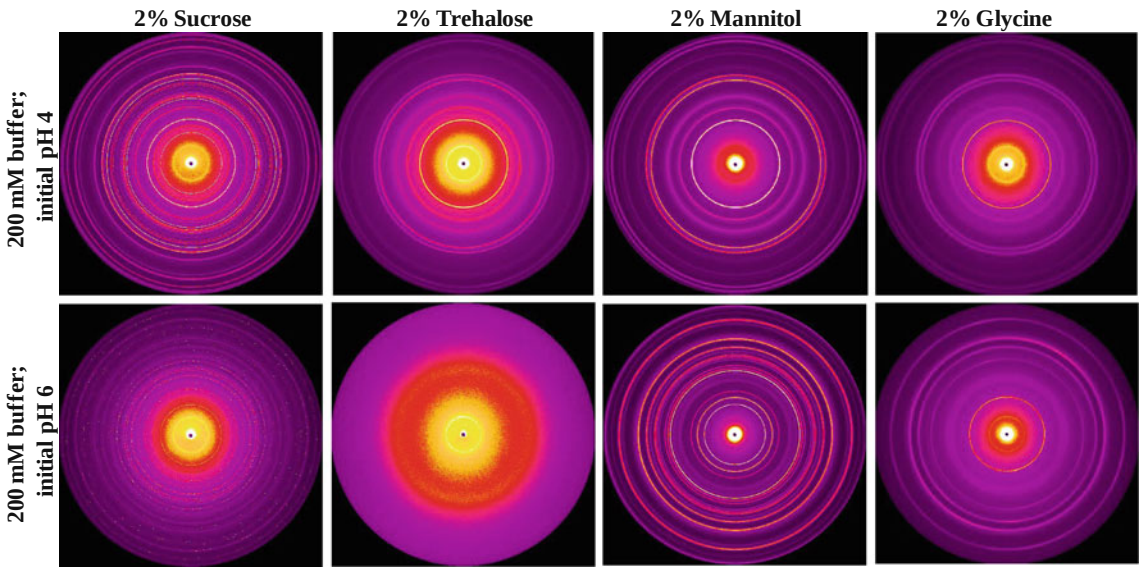

Fig. 11 Two-dimensional synchrotron XRD images of the final lyophiles prepared using the solutions containing succinic acid buffered to pH values 4.0 and 6.0 at RT. The solutions also contain cosolutes (sucrose, trehalose, mannitol or glycine).

ACKNOWLEDGEMENTS

The XRD studies were carried out in the College of Science and Engineering Characterization Facility, University of Minnesota, which receives partial support from NSF through the MRSEC program. The use of the Advanced Photon Source at Argonne National Laboratory through the Midwest Universities Collaborative Access Team (MUCAT sector) is gratefully acknowledged.

REFERENCES

1. Akers MJ, Defelippis MR. Peptides and proteins as parenteral solutions. In: Frokjaer S, Hovgaard L, editors. Pharmaceutical Formulation Development of Peptide and Proteins. Philadelphia: Taylor and Francis Inc.; 2003. p. 145–77.
2. Akers MJ, Fites AL, Robison RL. Formulation design and development of parenteral suspensions. J Parenter Sci Technol. 1987;41:88–96.
3. Akers MJ, Vasudevan V, Stickelmeyer M. Formulation development of protein dosage forms. In: Nail SL, Akers MJ, editors. Development and manufacture of protein pharmaceuticals. New York: Kluwer Academic/Plenum publishers; 2002. p. 47–127.
4. Defelippis MR, Akers MJ. Peptides and proteins as parenteral suspensions: An overview of design, development, and manufacturing considerations. In: Frokjaer S, Hovgaard L, editors. Pharmaceutical Formulation Development of Peptide and Proteins. Philadelphia: Taylor and Francis Inc; 2000. p. 113. 2003.
5. Pikal MJ. Freeze drying. In: Swarbrick J, editor. Encyclopedia of pharmaceutical technology, vol. 1. New York: Informa Healthcare; 2007. p. 1807–33.
6. Trissel LA. Handbook on injectable drugs. 14th ed. Bethesda: American Society of Health-System Pharmacists; 2007.
7. Shalaev EY. The impact of buffer on processing and stability of freeze-dried dosage forms, part 1: Solution freezing behavior. Am Pharm Rev. 2005;8:80–7.
8. Shalaev EY, Johnson-Elton TD, Chang L, Pikal MJ. Thermophysical properties of pharmaceutically compatible buffers at subzero temperatures: Implications for freeze-drying. Pharm Res. 2002;19:195–201.
9. van den Berg L. pH changes in buffers and foods during freezing and subsequent storage. Cryobiology. 1966;3:236–42.
10. van den Berg L, Rose D. Effect of freezing on the pH and composition of sodium and potassium phosphate solutions: The reciprocal system KH_2PO_4-Na_2HPO_4-H_2O. Arch Biochem Biophys. 1959;81:319–29.
11. Varshney DB, Sundaramurthi P, Shalaev EY, Kumar S, Kang S-W, Gatlin LA, *et al.* Phase transitions in frozen systems and during freeze-drying: Quantification using synchrotron X-ray diffractometry. Pharm Res. 2009;26:1064–75.
12. Pikal-Cleland KA, Cleland JL, Anchordoquy TJ, Carpenter JF. Effect of glycine on pH changes and protein stability during freeze-thawing in phosphate buffer systems. J Pharm Sci. 2002;91:1969–79.
13. Akers MJ. Excipient—drug interactions in parenteral formulations. J Pharm Sci. 2002;91:2283–300.
14. Sundaramurthi P, Shalaev E, Suryanarayanan R. "pH swing" in frozen solutions-consequence of sequential crystallization of buffer components. J Phys Chem Lett. 2010;1:265–8.
15. Sundaramurthi P, Shalaev E, Suryanarayanan R. Calorimetric and diffractometric evidence for the sequential crystallization of buffer components and consequent pH swing in frozen solutions. J Phys Chem B. 2010;114:4915–23.
16. Sundaramurthi P, Suryanarayanan R. Trehalose crystallization during freeze-drying: Implications on lyoprotection. J Phys Chem Lett. 2010;1:510–4.
17. Varshney DB, Kumar S, Shalaev EY, Sundaramurthi P, Kang S-W, Gatlin LA, *et al.* Glycine crystallization in frozen and freeze-dried systems: Effect of pH and buffer concentration. Pharm Res. 2007;24:593–604.
18. Sundaramurthi P, Patapoff TW, Suryanarayanan R. Crystallization of trehalose in frozen solutions and its phase behavior during drying. Pharm. Res. 2010, doi:10.1007/s111095-010-0243-2.
19. Yalkowsky SH, He Y. Handbook of aqueous solubility data. New York: CRC press; 2003.
20. Chongprasert S, Knopp SA, Nail SL. Characterization of frozen solutions of glycine. J Pharm Sci. 2001;90:1720–8.
21. Kasraian K, Spitznagel TM, Juneau JA, Yim K. Characterization of the sucrose/glycine/water system by differential scanning calorimetry and freeze-drying microscopy. Pharm Dev Technol. 1998;3:233–9.
22. Li X, Nail SL. Kinetics of glycine crystallization during freezing of sucrose/glycine excipient systems. J Pharm Sci. 2005;94:625–31.
23. Pyne A, Suryanarayanan R. Phase transitions of glycine in frozen aqueous solutions and during freeze-drying. Pharm Res. 2001;18:1448–54.
24. Yu L, Ng K. Glycine crystallization during spray-drying: The pH effect on salt and polymorphic forms. J Pharm Sci. 2002;91:2367–75.
25. Chang BS, Randall CS. Use of subambient thermal analysis to optimize protein lyophilization. Cryobiology. 1992;29:632–56.
26. Sundaramurthi P, Suryanarayanan R. Influence of crystallizing and non-crystallizing cosolutes on trehalose crystallization during freeze-drying. Pharm. Res. 2010, doi:10.1007/s111095-010-0221-8.
27. Pikal-Cleland KA, Rodriguez-Hornedo N, Amidon GL, Carpenter JF. Protein denaturation during freezing and thawing in phosphate buffer systems: Monomeric and tetrameric beta -galactosidase. Arch Biochem Biophys. 2000;384:398–406.
28. Sundaramurthi P, Suryanarayanan R. Predicting the crystallization propensity of carboxylic acid buffers in frozen systems—relevance to freeze-drying J. Pharm. Sci. 2010, in press.
29. Telang C, Yu L, Suryanarayanan R. Effective inhibition of mannitol crystallization in frozen solutions by sodium chloride. Pharm Res. 2003;20:660–7.
30. Telang C, Suryanarayanan R, Yu L. Crystallization of D-mannitol in binary mixtures with NaCl: Phase diagram and polymorphism. Pharm Res. 2003;20:1939–45.
31. Izutsu K-i, Ocheda SO, Aoyagi N, Kojima S. Effects of sodium tetraborate and boric acid on nonisothermal mannitol crystallization in frozen solutions and freeze-dried solids. Int J Pharm. 2004;273:85–93.
32. Izutsu K-i, Yomota C, Aoyagi N. Inhibition of mannitol crystallization in frozen solutions by sodium phosphates and citrates. Chem Pharm Bull. 2007;55:565–70.
33. Powder Diffraction File. Hexagonal ice, card # 00-042-1142; D-trehalose dihydrate, card # 00-029-1955; β-succinic acid, card # 00-031-1899; monosodium succinate, card # 00-030-1927; sucrose, card # 00-024-1977; β-D-Glucose 00-039-1837; β-D-mannitol, card #00-022-1797; δ-D-mannitol, card # 00-022-1794. International Centre for Diffraction Data, Newtown Square, PA; 2004.